SCIENTIFIC REPORTS

OPEN

SUBJECT AREAS:
PHARMACOLOGY
CELL ADHESION
MOLECULAR BIOLOGY
CANCER PREVENTION

Received
5 December 2013

Accepted
24 February 2014

Published
11 March 2014

Correspondence and requests for materials should be addressed to J.W.S. (shaojingwei@fzu.edu.cn) or L.J. (pharmlink@gmail.com)

Nitric Oxide Inhibits Hetero-adhesion of Cancer Cells to Endothelial Cells: Restraining Circulating Tumor Cells from Initiating Metastatic Cascade

Yusheng Lu[1], Ting Yu[1], Haiyan Liang[1], Jichuang Wang[1], Jingjing Xie[1], Jingwei Shao[1], Yu Gao[1], Suhong Yu[1], Shuming Chen[2], Lie Wang[2] & Lee Jia[1]

[1]Cancer Metastasis Alert and Prevention Center, College of Chemistry and Chemical Engineering, Fuzhou University, Fuzhou 350002, China, [2]Surgery Department, Fuzhou General Hospital, Fuzhou, 350025, China.

Adhesion of circulating tumor cells (CTCs) to vascular endothelial bed becomes a crucial starting point in metastatic cascade. We hypothesized that nitric oxide (NO) may prevent cancer metastasis from happening by its direct vasodilation and inhibition of cell adhesion molecules (CAMs). Here we show that S-nitrosocaptopril (CAP-NO, a typical NO donor) produced direct vasorelaxation that can be antagonized by typical NO scavenger hemoglobin and guanylate cyclase inhibitor. Cytokines significantly stimulated production of typical CAMs by the highly-purified human umbilical vein endothelial cells (HUVECs). CAP-NO inhibited expression of the stimulated CAMs (particularly VCAM-1) and the resultant hetero-adhesion of human colorectal cancer cells HT-29 to the HUVECs in a concentration-dependent manner. The same concentration of CAP-NO, however, did not significantly affect cell viability, cell cycle and mitochondrial membrane potential of HT-29, thus excluding the possibility that inhibition of the hetero-adhesion was caused by cytotoxicity by CAP-NO on HT-29. Hemoglobin reversed the inhibition of CAP-NO on both the hetero-adhesion between HT-29 and HUVECs and VCAM-1 expression. These data demonstrate that CAP-NO, by directly releasing NO, produces vasorelaxation and interferes with hetero-adhesion of cancer cells to vascular endothelium via down-regulating expression of CAMs. The study highlights the importance of NO in cancer metastatic prevention.

The ability to metastasize is a hallmark of malignant tumors, and metastasis is the principal cause of death among cancer patients[1,2]. The root cause of cancer metastasis can be traced down to the presence of circulating tumor cells (CTCs) in blood[3]. High CTC number in blood correlates with aggressive disease, increased metastasis, and decreased time to relapse[4]. The formation of initial micrometastatic foci is proposed to depend on a series of consequential events, including the activation of dormant CTCs, interaction and adhesion between CTCs and vascular endothelial bed of secondary organs, and the continued survival and initial proliferation after extravasation. Adhesion of CTCs to vascular endothelium becomes a crucial starting point of metastasis that precedes invasion and extravasation of CTCs, and formation of micrometastasis foci. Cell adhesion molecules (CAMs) expressed by endothelial cells may play an important role in attracting CTCs to the endothelial cells. Increasing evidences suggest that CTC adhesion to the endothelial cells is influenced by endothelial activation or tissue-specific differences in endothelial cells[5], and depends on the expression of specific cell surface molecules[5–7]. Previous study revealed that several cytokines, including tumor necrosis factor alpha (TNF-α) and interleukin-1 beta (IL-1β), up-regulated the expression of CAMs in endothelial cells[8]. CTC surface α4β1 integrin mediated adhesion of CTCs to vascular endothelium by interaction with the N-terminal domains of inducible cell adhesion molecules 110/vascular cell adhesion molecule-1 (INCAM-110/VCAM-1)[9]. E-selectin on endothelial cells has been identified as tumor cell surface CD44v4 and sialyl lewis x (sLe^x)[10,11]. The intercellular adhesion molecule-1 (ICAM-1) was expressed on endothelial cells and recognized as the β2 integrin[12]. Treatment of human umbilical vein endothelial cells (HUVECs) with monoclonal anti-E-selectin, anti-ICAM-1, and anti-VCAM-1 antibodies had a significant effect on the adhesion of leukemia cells or cancer cells to HUVECs[13,14]. Therefore, we hypothesized that if we could chemically interfere with the adhesion of CTCs to

vascular endothelial cells of the distant metastatic tissues (the most important and first step of metastatic cascade), we may efficiently prevent cancer metastatic cascade from initiation.

Nitric oxide (NO) plays important roles in the cardiovascular system. It was first discovered as the endothelium-derived relaxing factor (EDRF)[15,16]. Endothelial NO also limits platelet activation, adhesion, and aggregation[17]. NO relaxes both vascular and nonvascular smooth muscles[18,19], limits proliferation of vascular smooth muscle cells[20], and inhibits adhesion of leukocyte to the endothelium[21,22]. NO also sensitizes tumor cells to chemotherapeutic compounds[23]. In addition, various direct and indirect mechanisms have been proposed for the antitumor activities of NO[24].

S-nitrosocaptopril (CAP-NO) is the S-nitrosylated Captopril (CAP) that possesses dual pharmacological properties of both NO and angiotensin-converting enzyme inhibitor (ACEI, i.e., Captopril)[25], which was first discovered by Joseph Loscalzo[26]. CAP-NO exhibits many NO-like activities such as direct vasorelaxation in vivo and in vitro[25,27], and inhibition of platelet aggregation[26]. Because of the above-mentioned beneficial effects of NO in preventing adhesion of CTCs to vascular endothelium, the present study was designed to explore the possible inhibitory role of CAP-NO on hetero-adhesion between cancer cells and vascular endothelial cells in response to various cytokine exposures, and investigate the corresponding mechanisms of action related to the vasorelaxation and adhesion inhibition by CAP-NO.

Results

EDRF-like activity of CAP-NO. When added to rabbit aortic rings that had been precontracted submaximally with phenylephine, CAP-NO caused instantaneous vasorelaxation in a dose-dependent manner (Fig. 1)[28]. The threshold CAP-NO concentration that produces vasorelaxation was approximately 1 nM. CAP-NO produced 100% relaxation on the isolated blood vessels at 100 nM. Unlike authentic NO that only produced a 5-min transient relaxation when 75 nM of NO was added to isolated blood vessels[29], CAP-NO produced a vasorelaxation that persisted for more than 1 h. In order to investigate whether the vasorelaxation induced by CAP-NO was attributable to NO release from the compound, bovine hemoglobin (Hb) and 1H-[1, 2, 4] oxadiazolo [4, 3,-a] quinoxalin-1-one (ODQ) were added separately to the rabbit aortic rings when CAP-NO produced its maximal relaxation of the rings. Addition of Hb (10 μM) immediately reversed the CAP-NO-induced vasorelaxation (Fig. 1). This observation is attributed to the rapid inactivation of EDRF/NO by Hb[30]. When ODQ (10 μM) was added to the aortic rings during the CAP-NO-induced relaxation, rapid reversal of the relaxation was also observed (Fig. 1). Those results suggest that CAP-NO induces vasorelaxation by releasing NO and activating the sGC/cGMP pathway.

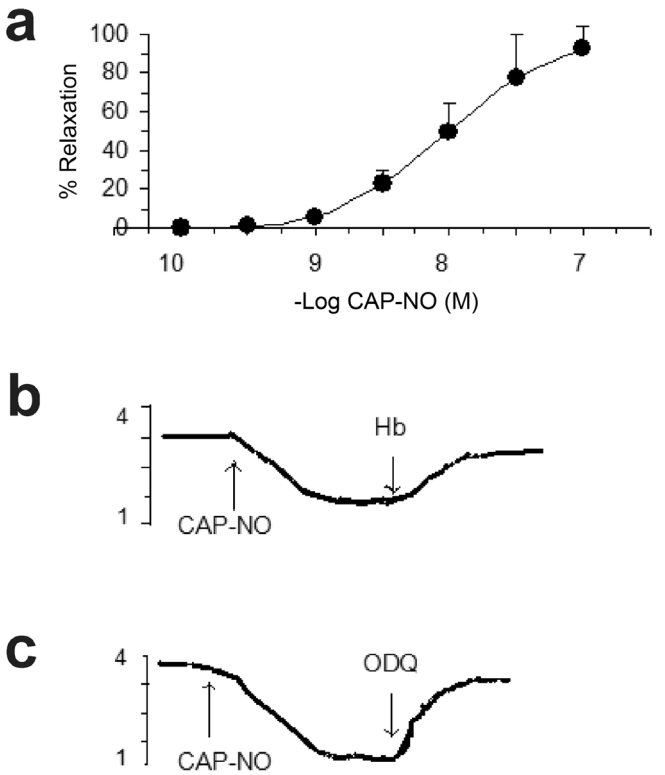

Figure 1 | Vasorelaxation of CAP-NO and the related mechanism of action. (a) Dose-dependent relaxation caused by CAP-NO in rabbit aortic rings precontracted with phenylephine. The lower panels (b) and (c): reversal of CAP-NO-induced (100 nM) relaxation of rabbit aortic rings by Hb (10 μM) and ODQ (10 μM). The y-axis represents the vascular tension in gram. Results are presented as the mean ± SD. (n = 4).

HUVECs characterization. HUVECs were successfully separated and cultured as described before[31]. The cells were homogenous with centrally-located nucleus and indistinct cell borders. They exhibited typical cobblestone growth pattern of endothelial cells (Fig. 2a). When maintained at confluence for an extended period of time, HUVECs became tightly packed but show no tendency to overlap or overgrow one another (Fig. 2b). CD31 (platelet and endothelial cell adhesion molecule-1, PECAM) and CD144 (Vascular-Endothelial cadherin, VE-Cadherin) are considered good biomarkers of endothelial cells[32–34]. The HUVECs that we isolated were over 99% of CD31 and CD144 positive detected by the flow cytometric assay (Fig. 2c and 2d), indicating high purity of the HUVECs.

Adhesion molecule activation analysis. In the resting state, we found that the HUVECs expressed ICAM-1 (intercellular adhesion molecule-1, CD54), but not E-selectin (CD62E), or VCAM-1 (vascular cell adhesion molecule-1, CD106). The result coincides with previous reports[8,35]. Following stimulation of the HUVECs by IL-1β (1 ng/mL), TNF-β (10 ng/mL), TNF-α (10 ng/mL), IL-6 (10 ng/mL), IFN-γ (10 ng/mL), endothelial cell growth supplement (ECGS, 100 μg/mL) and fibronectin (100 ng/mL) for 4 h, expression of CD54, CD62E and

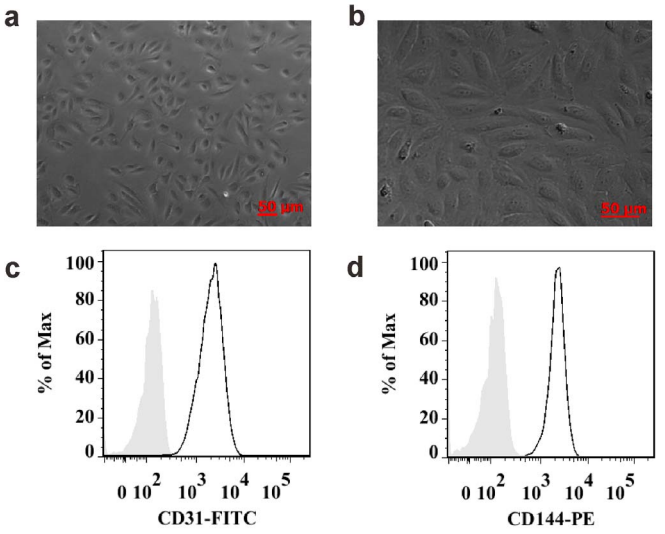

Figure 2 | Identification and characterization of HUVECs. (a and b) Microscopic morphology: exhibited typical cobblestone growth pattern of endothelial cells (a), HUVECs become tightly packed but show no tendency to overlap or overgrow one another (b). (c and d) HUVECs purity was assessed by flow cytometry: CD31, 99.5%; and CD144, 99.6%, compared with isotype control (silver area).

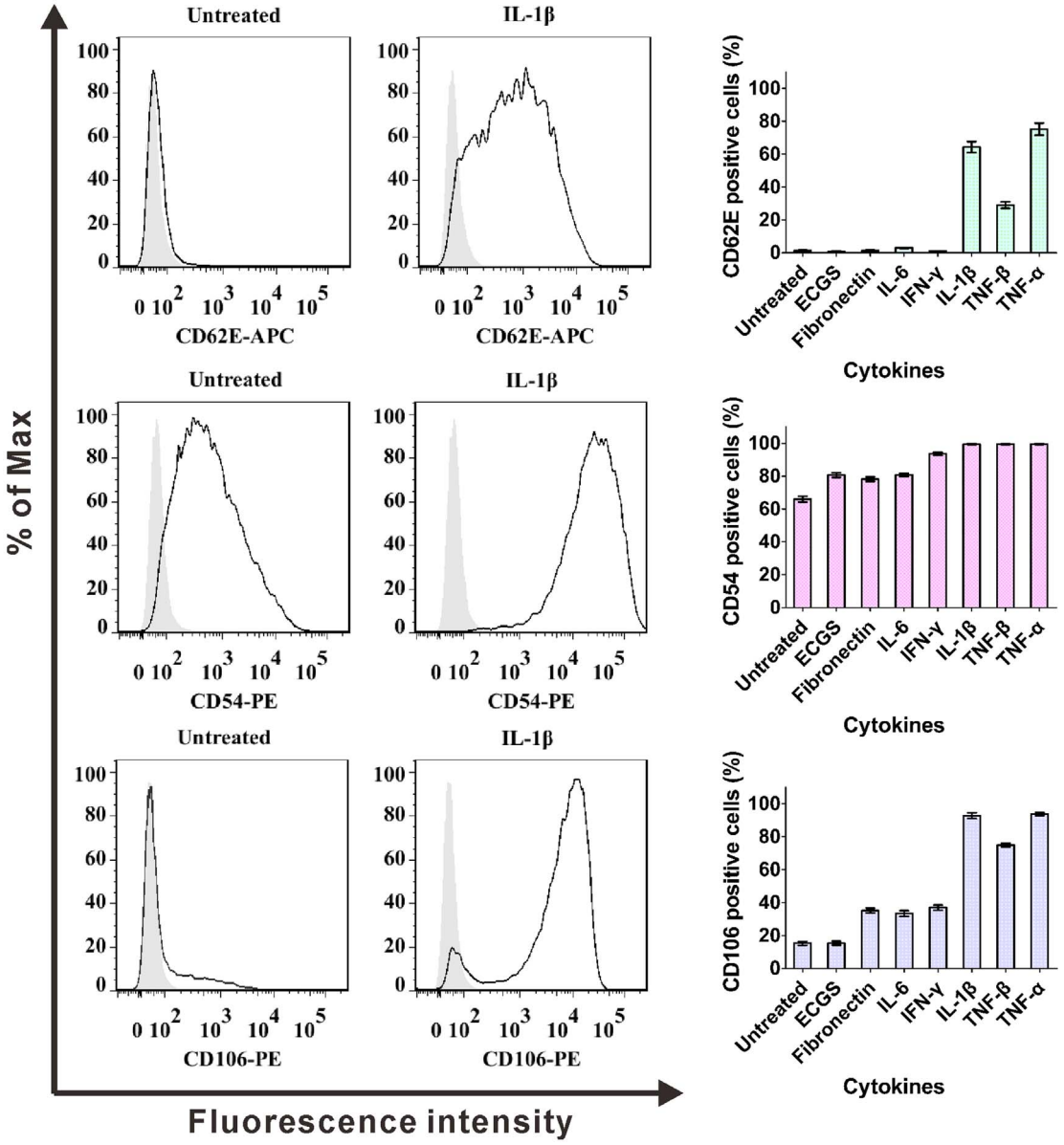

Figure 3 | Flow cytometric analysis of cytokine-stimulated CD62E (E-selectin), CD54 (ICAM-1) and CD106 (VCAM-1) expression by HUVECs. HUVECs was cultivated with IL-1β (1 ng/mL), TNF-β (10 ng/mL), TNF-α (10 ng/mL), IL-6 (10 ng/mL), IFN-γ (10 ng/mL), ECGS (100 μg/mL) and fibronectin (100 ng/mL), respectively, for 4 h. Expression of CD62E, CD54 and CD106 were detected by flow cytometry using silver area as isotype controls. Bar graph shows the percentage of positive cells (right panels), contour polt analysis (left panels) shows $CD62E^+$, $CD54^+$ and $CD106^+$ cells, in comparison with isotype controls. Bars represent the mean ± SEM (n = 3).

CD106 by the HUVECs was significantly up-regulated by IL-1β, TNF-β and TNF-α respectively (Fig. 3). IL-6, IFN-γ, ECGS and fibronectin did not significantly stimulate endothelial CD62E expression. However, they up-regulated expression of CD54. IL-6, IFN-γ and fibronectin slightly increased endothelial expression of CD106 (Fig. 3). The results were summarized in Supplementary Table S1. Experiments showed that the endothelial cells had difference sensitivity when stimulated by different cytokines.

CAP-NO inhibited adhesion of HT-29 cells to HUVECs. Before the cell adhesion assay, we examined if CAP-NO itself had an effect on spontaneous adhesion of HT-29 cells to the bottom of the culture plate. The data showed that CAP-NO, up to 100 μM, did not produce a significant effect on the spontaneous adhesion of HT29 cells to the culture plate (Fig. 4a). According to the present study results, IL-1β seemed to be potent in activating the adhesion molecules. We therefore pretreated HUVECs with IL-1β (1 ng/mL) for 4 h before co-incubation of the HUVECs with fluorescence-labeled HT-29. Quantification of HT-29 adhered to the HUVECs was determined by fluorescence-labeled cell counts, which showed that CAP-NO (0.5, 5 and 50 μM) interfered the adhesion of HT-29 cells to HUVECs in a dose-dependent manner. In the presence of CAP-NO (0.5, 5 and 50 μM) for 1 h, the adhesion between HT-29 and HUVECs was reduced from 92.4 ± 2.8, 69.2 ± 2.4 to 61.5 ± 2.1% ($P < 0.01$), respectively, compared to the IL-1β-treated HUVECs control. Moreover, 12 h treatment with CAP-NO reduced the adhesion from 69.6 ± 3.0 (0.5 μM), 56.4 ± 1.7 (5 μM) to 42.8 ± 0.5% (50 μM). In comparison to CAP-NO, CAP did not interfere the adhesion of HT-29 to the HUVECs (Fig. 4b–d).

Cytotoxic effects of CAP-NO on HT-29 cells and HUVECs. CAP-NO had weak cytotoxicity on HT-29 cells. Exposures of HT-29 to

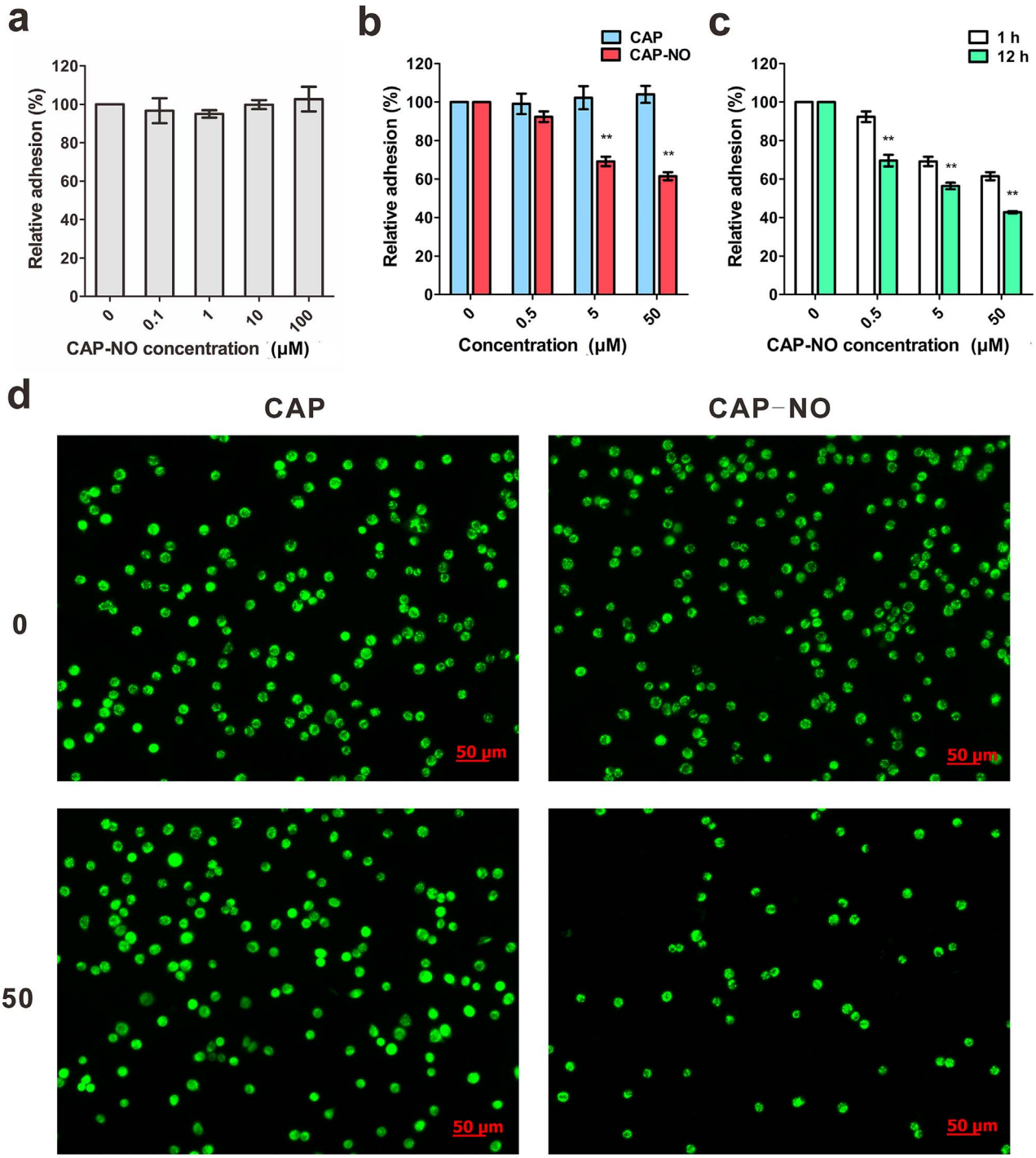

Figure 4 | CAP-NO inhibited adhesion of HT-29 cells to HUVECs. (a) Effect of CAP-NO on the spontaneous adhesion of HT-29 cells to culture plate within 1 h observation. (b) Quantification of HT-29 adhered to the HUVEC monolayers in the presence and absence of CAP-NO or CAP. (c) Effects of CAP-NO on adhesion of HT-29 to HUVECs at indicated time points. The % relative adhesion was determined by fluorescence-labeled cell count assay, and the results are based on the IL-1β stimulated HUVECs. (d) Rhodamine 123-labeled HT-29 cells were added to the HUVEC monolayers stimulated by IL-1β (1 ng/mL) in the presence and absence of CAP-NO or CAP (both 50 μM). Fluorescence microscopy showed HT-29 cells (green) adhered to the HUVECs. Bars represent the mean ± SEM (n = 3); ** indicates $P < 0.01$.

CAP-NO at concentrations ranging from 0.1 μM to 1000 μM could not reach the inhibitory IC_{50} values of CAP-NO, indicating that the IC_{50} was greater than 1000 μM, which was consistent with our previous report[23]. By comparison, the HUVECs showed a similar sensitivity to CAP-NO (Fig. 5a). Cell cycle analysis further supported that CAP-NO, even at 100 μM, did not have a significant inhibition on cell cycle distribution of HT-29 (Fig. 5b). 3, 3-dihexyloxacarbocyanine iodide (DiOC6(3)) was used as a mitochondrion-specific and voltage-dependent dye for determining mitochondrial membrane potential ($\Delta\psi_m$). Increase in $\Delta\psi_m$ will lead to mitochondrial dysfunction and result in apoptosis. A significant increase by 125.6 ± 1.8% in $\Delta\psi_m$ of HT-29 was observed only when CAP-NO concentration was up to 1000 μM (Fig. 5c and 5d). The data suggested that mitochondrial

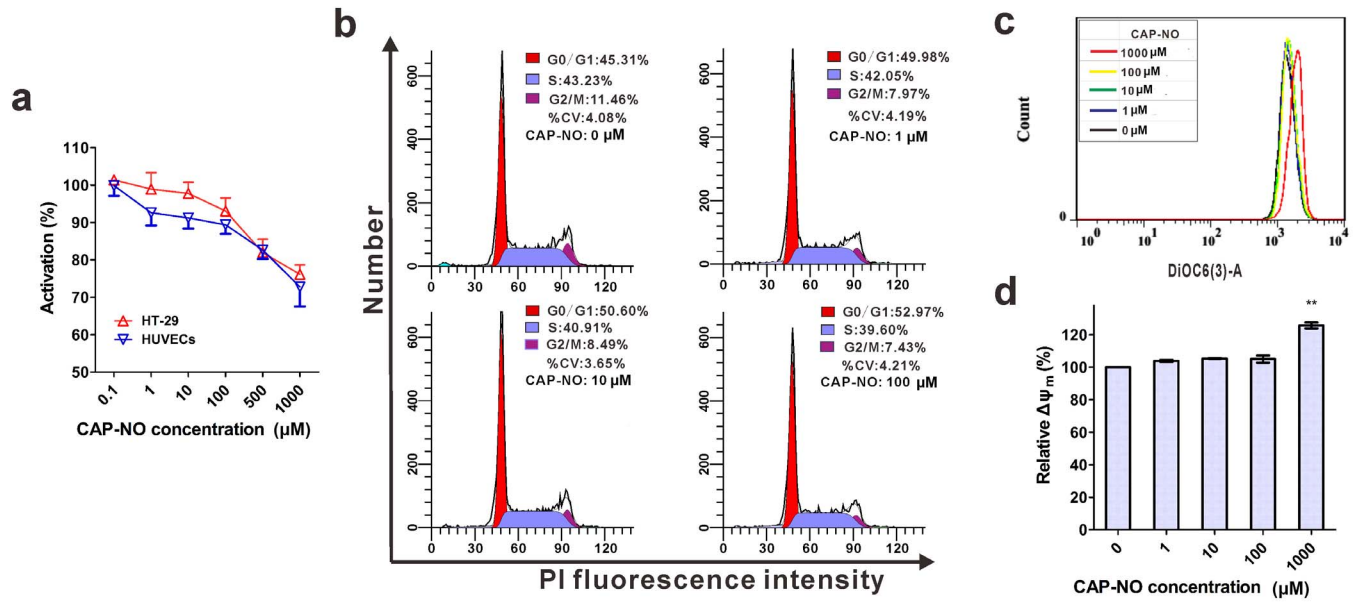

Figure 5 | Inhibitory effects of CAP-NO. (a) The HT-29 cells and HUVECs were separately exposed to different concentrations of CAP-NO for 24 h. The cytotoxicity was determined by MTT assay and expressed as the percentage of the controls. (b) Effect of CAP-NO on cell cycle. HT-29 cells were incubated with CAP-NO (0, 1, 10 and 100 μM) for 24 h. The cell cycle was assessed by flow cytometry. Cell cycle distribution was analyzed using the Modfit software, CVs <8% are recommended for useful S-Phase determination. (c and d) Effect of CAP-NO on $\Delta\psi_m$. HT-29 cells were exposed to CAP-NO (1, 10, 100 and 1000 μM) for 12 h, respectively. The $\Delta\psi_m$ was determined by flow cytometry. $\Delta\psi_m$ levels of HT-29 cells were expressed as the mean fluorescence intensities and calculated as percentage of controls. Bars represent the mean ± SEM (n = 3); ** indicates $P < 0.01$.

dysfunction is involved in the apoptosis induced by high concentration of CAP-NO.

Down-regulation by CAP-NO of adhesion molecule expression. The effects of CAP-NO and CAP on expression by HUVECs of E-selectin, ICAM-1 and VCAM-1 were determined by flow cytometry. The HUVECs were pretreated with 1 ng/mL IL-1β for 4 h, followed by treatment of the HUVECs with CAP-NO or CAP for 12 h. CAP-NO, in a dose-dependent manner, down-regulated ICAM-1 expression by 83.2 ± 0.9 (1 μM), 74.2 ± 3.6 (10 μM) and 70.3 ± 1.5% (100 μM). By comparison, CAP (1, 10 and 100 μM) did not show significant dose-dependent down-regulation of ICAM-1 expression (87.4 ± 0.8, 86.9 ± 1.0 and 86.0 ± 1.3%, respectively). In addition, there were significant differences between CAP-NO and CAP in their down-regulation of ICAM-1 expression (Fig. 6a). The difference indicated that the down-regulation of ICAM-1 expression was induced by NO.

CAP-NO and CAP (1, 10 and 100 μM) caused a dose-dependent down-regulation of E-selectin expression induced by IL-1β. CAP-NO was more potent than CAP in this regard ($P < 0.05$; Fig. 6b). The effect did not seem to be time-dependent (Fig. 6d).

Flow cytometric analysis revealed that CAP-NO at 1, 10 and 100 μM caused a significant decrease in VCAM-1 expression by 35.2 ± 1.4, 36.6 ± 1.7 and 33.3 ± 2.6%, respectively, compared to the IL-1β stimulated cells. However, CAP (1, 10 and 100 μM) had no significant effect on VCAM-1 expression (Fig. 6c and 6e), indicating that the down-regulation of VCAM-1 expression was caused by the NO moiety of CAP-NO.

Integrin β1 (CD29) is an adhesion ligand expressed on HT-29 cells. Flow cytometric analysis showed that CAP-NO had no significant effect on integrin β1 expression on HT-29 cells determined at the incubation time points of 1, 4 and 24 h (Fig. 6f).

To further confirm the role of CAP-NO in down-regulating expression of adhesion molecules observed by flow cytometry, western blot analysis was performed. Expression of VCAM-1 was very low in both the control and the IFN-γ-stimulated HUVECs, but high in the IL-1β-stimulated HUVECs. Pretreatment of the HUVECs with CAP-NO at 1, 10 and 100 μM significantly inhibited VCAM-1 expression by 69.6 ± 2.0, 35.9 ± 3.8 and 42.5 ± 1.7%, respectively, compared to the IL-1β stimulated cells (Fig. 6g and 6h). The result was consistent with that obtained from the flow cytometric analysis.

Discussion

The present study clearly demonstrated, for the first time, that the NO donor CAP-NO could interfere with the hetero-adhesion between the typical human cancer cells and endothelial cells. The inhibition on the adhesion was CAP-NO concentration dependent, and clearly related to the NO moiety in the structure of CAP-NO. It is the NO moiety that down-regulated expression of CAMs, starting at CAP-NO concentration as low as 5 μM without significantly affecting the viability of cancer cells.

Various cytokines stimulate expression of CAMs by endothelial cells with different potency. The present study used the flow cytometry to rank the potency of these cytokines in stimulating CAMs expression by HUVECs. We demonstrated that IL-1β, TNF-α, and TNF-β significantly stimulate the typical CAMs, i.e., E-selectin, VCAM-1 and ICAM-1, expressed by the HUVECs (Fig. 3). The result is in line with that reported by others[8]. By comparison, IL-6, IFN-γ, ECGS and fibronectin did not significantly stimulate expression by the HUVECs of E-selectin, ICAM-1 and VCAM-1. As a result, we chose the most potent cytokine IL-1β (1 ng/mL) as a tool molecule in the present study to investigate the effect of CAP-NO on adhesion between HT-29 cancer cells and HUVECs.

CAP-NO inhibited expression by the HUVECs of E-selectin, ICAM-1 and VCAM-1 induced by IL-1β in a dose-dependent manner. The significant inhibition by CAP-NO can be observed at its concentration as low as 1 μM ($P < 0.01$; Fig. 6), resulting in the inhibition by CAP-NO on hetero-adhesion between HT-29 and the HUVECs (Fig. 4). By parallel comparison, CAP did not show the same effects as CAP-NO did. In addition, pretreatment of the co-incubation system with NO scavenger Hb (1 μM) for 5 min reversed the inhibition of CAP-NO on both the hetero-adhesion between HT-29 and the HUVECs (Fig. 7a) and IL-1β-induced VCAM-1 expression (Fig. 7b).

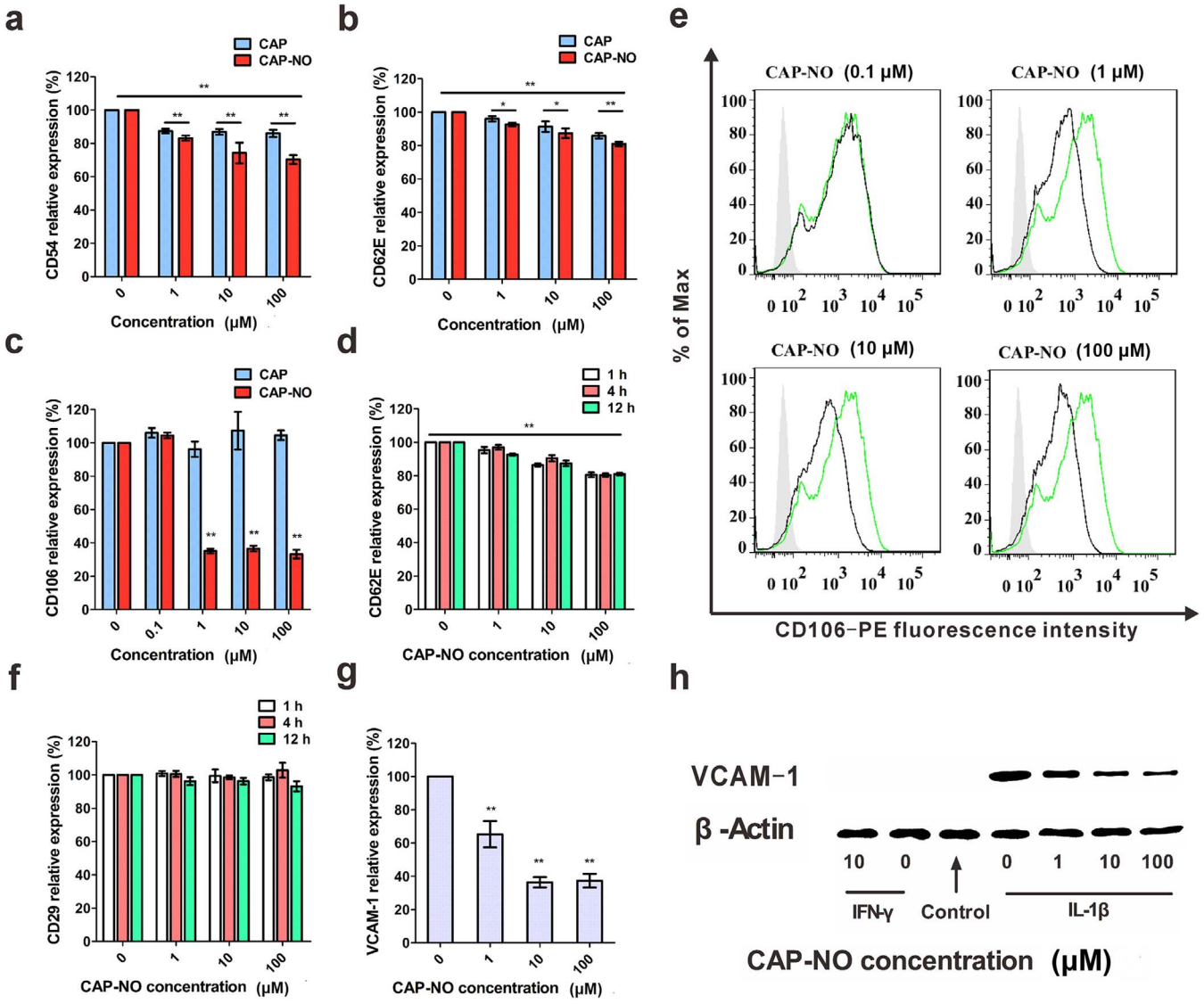

Figure 6 | Flow cytometric and western blot analyses of effects of CAP-NO and CAP on CAMs. HUVECs were pretreated with 1 ng/mL IL-1β for 4 h followed by incubation with CAP-NO or CAP for another 12 h (unless otherwise stated). Flow cytometric analysis showed significant inhibition by CAP-NO on expression induced by IL-1β (1 ng/mL) of ICAM-1 (a), E-selectin (b), and VCAM-1 (c). Results are expressed as the mean fluorescence intensities and calculated as percentage of controls. (d) Effects of CAP-NO on E-selectin expression at indicated time points. (e) Expression of VCAM-1 determined by flow cytometry using green curve as a control (IL-1β only), and silver area is an isotype control. (f) Effects of CAP-NO on CD29 expression at indicated time points. (g and h) Western blot analysis of VCAM-1 expression by HUVECs pretreated with IFN-γ (10 ng/mL) or IL-1β (1 ng/mL) for 4 h followed by incubation with CAP-NO (0, 1, 10 and 100 μM) for another 12 h. Band intensity was quantified by using Image Lab analysis software, and calculated as percentage of controls (IL-1β only). Bars represent the mean ± SEM (n = 3); *, $P < 0.05$, and ** $P < 0.01$.

These results collectively demonstrated that it is the NO moiety that inhibits the hetero-adhesion between HT-29 and the HUVECs.

The mechanisms of actions of CAP-NO can be summarized as follows since its discovery in 1989[26]: 1) inhibition of platelet activation and aggregation[26,36]; 2) direct vasorelaxation[37–39] including vasorelaxation of cerebral capillary[19]; 3) inhibition of angiotensin converting enzyme and direct antagonization against effect of formed angiotensin II[26]; 4) decrease in hypertension induced by NOS inhibitor N^G-monomethyl-L-arginine, and by a two-kidney one-clipped Goldblatt method[25]; decrease in hypertension of spontaneous hypertensive rats and Dahl salt-sensitive hypertensive rats[40]; 5) antiangiogenic effect[41]; 6) partially by inhibiting the expression of VCAM and ICAM[42,43]; 7) enhancement in transcellular permeability of Taxol[23]; 8) as a potent radiosensitizer used in combination with chemotherapy because it could increase blood flow and oxygen consumption of a tumor[44].

The beneficial effects of CAP-NO in preventing CTCs from adhesion, invasion to endothelial bed and the resultant micrometastatic foci may attribute to its collective actions (Fig. 8). Extensive experimental evidence shows that platelets support cancer metastasis[45]. Within the circulation system, platelets guard cancer cells from immune elimination, promote their arrest on the endothelium, and support the establishment of secondary lesions. CAP-NO is well demonstrated to have an inhibitory effect on platelet activation. Moreover, the vasorelaxation effect of CAP-NO, which was demonstrated in the present study to be related to the release of NO from CAP-NO (Fig. 1), could make the diameter of capillaries larger to prevent CTCs from trapped there, an event often occurring in cancer metastasis[4]. Unlike the traditional cytotoxic compounds that kill cancer cells at their concentrations as low as micromole levels that would produce many intolerable side effects, NO donor molecules

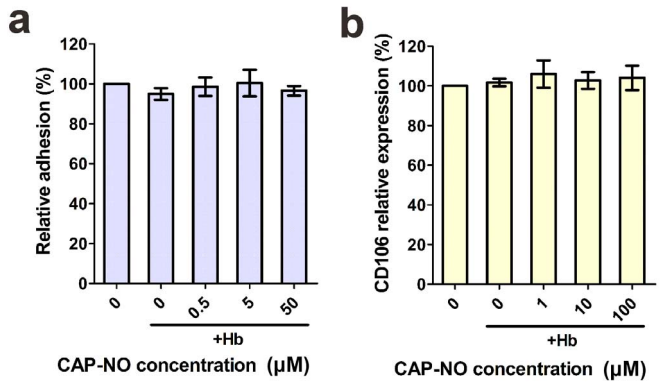

Figure 7 | NO scavenger Hb reversed the inhibitory effect of CAP-NO on the hetero-adhesion between HT-29 and HUVECs and -induced expression of VCAM-1 in the presence of IL-1β (1 ng/mL). (a) 5-min pretreatment with Hb (1 μM) reversed the inhibition CAP-NO on the IL-1β-induced adhesion determined by fluorescence-labeled cell count assay. (b) Hb also reversed IL-1β-induced expression of VCAM-1 (CD106). Results are expressed as the mean fluorescence intensities and calculated as percentage of controls (IL-1β only). Bars represent the mean ± SEM (n = 3).

often exhibit their cytostatic effects at concentrations 30–100 μM or higher on the 9 human cancer subpanels of 60 human cell lines[46].

In conclusion, the present study demonstrated that CAP-NO had weak cytotoxicity against HT29 cancer cells. CAP-NO interfered with the hetero-adhesion between cancer cells and HUVECs by down-regulation of CAMs induced by cytokines. This newly-discovered activity of CAP-NO makes it best-suited for a cancer metastatic chemopreventive in addition to its other beneficial effects in this regard.

Methods

Reagents, animals and human samples. The preparation and physicochemical characterization of crystalline CAP-NO were described previously[41,47]. ODQ and Hb were purchased from Sigma (St. Louis, MO). Human interleukin-1 beta (IL-1β), human interferon gama (IFN-γ), human tumor necrosis factor alpha (TNF-α), human lymphotoxin (LT, TNF-β) and mouse anti-human beta-actin (β-actin) antibody were purchased from Cell Signaling Technology, Inc. Recombinant human interleukin-6 (IL-6) was purchased from Peprotech, Inc. Mouse anti-human CD144-PE (P-phycoerythrin), mouse anti-human CD31-FITC (fluorescein isothiocyanate), mouse anti-human CD54-PE, mouse anti-human CD62E-APC (allophycocyanin), mouse anti-human CD29 (integrin β1)-PE, PE mouse IgG1 kappa isotype control, FITC mouse IgG1 kappa isotype control and APC mouse IgG1 kappa isotype control antibody were obtained from Becton Dickinson (BD) Pharmingen™. Mouse anti-human CD106-PE was obtained from eBioscience. Fibronectin and ECGS were obtained from BD Biocoat™. Rabbit anti-human VCAM-1 antibody was obtained from Abcam. Fluorescent dyes propidium iodide (PI) and DiOC6 (3) were obtained from Sigma-Aldrich. Protocols involving animal and human samples were approved by the Institute Animal Care and Use Committees in compliance with USDA regulations (National Research Council 1996).

Preparation of rabbit aortic rings for bioassay of NO activity. We used the standard isolated aortic ring assay to confirm CAP-NO's authenticity as an NO donor[30]. The rabbit aortic ring assay was conducted as previously described[29]. Briefly, a male New Zealand rabbit was euthanized by intravenous injection of sodium pentobarbital into a marginal ear vein. The descending thoracic aorta was quickly removed. The aortic rings (2 mm in length) were prepared and mounted in 20 mL of Krebs' solution (bubbled with 95% O_2/5% CO_2, 37°C) in organ chambers. Tension was measured isometrically, using Grass FTO3C transducers, and was displayed on model 7 Grass polygraphs. Rings were allowed to equilibrate for at least 90 min before experiments were initiated. Basal tension was maintained at approximately 3 g. To allow studies on relaxation, each ring was precontracted submaximally by addition of 50–100 nM phenylephine to the bathing solution. When the contraction had reached a steady state, CAP-NO was added to the bathing solution until the maximal relaxation was obtained. Hb (a typical NO scavenger) and ODQ (a should guanylate cyclase inhibitor) were also added to the bathing solution to investigate the mechanisms of action of CAP-NO[48].

Cell culture. Human colorectal cancer cell line HT-29 was obtained from Cell Bank of Chinese Academy. The cells were cultured in McCOY's 5A (Sigma-Aldrich) medium supplemented with 10% fetal bovine serum (FBS, obtained from Gibco), 100 units/mL penicillin and 100 μg/mL streptomycin at 37°C in a humidified atmosphere of 5% CO_2 and 95% air.

Isolation and culture of HUVECs. HUVECs were collected from human umbilical cord veins by minor modifications of previously described protocols[31]. HUVECs were isolated from human umbilical veins that were cannulated, perfused with Hanks' solution (8 g/L NaCl, 0.4 g/L KCl, 0.06 g/L KH_2PO_4, 0.126 g/L $Na_2HPO_4.12H_2O$, 0.35 g/L $NaHCO_3$, 1 g/L D-glucose) to remove blood, and then incubated with 0.1% type I collagenase (life technology) for 15–20 min at 37°C. After removal of type I collagenase, cells were maintained in 1% gelatin-coated tissue culture flasks in M199 (Gibco) medium supplemented with 20% FBS, 8 units/mL heparin, 100 μg/mL ECGS, 100 units/mL penicillin and 100 μg/mL streptomycin. The cells were cultured in a humidified atmosphere of 5% CO_2 and 95% air. HUVECs were not used after 6 passages.

Flow cytometry. Flow cytometric analysis was performed on a BD FACSAriaIII cell sorter with laser excitation set at 488 and 633 nm. The BD FACSDiva software provided with the system was employed for data acquisition and initial data analysis. Forward versus side scatter histograms were used to gate on single intact cells. The data was collected in FCS format with the subsequent analysis based on 10,000 cells to meet the light scatter criteria. PE, FITC, PI and DiOC6 (3) dyes were excited by 488 nm laser, with the PE (or PI) and FITC (or DiOC6 (3)) derived fluorescence detected through 585 and 530 nm bandpass filters, respectively. APC dye was excited by 633 nm laser, and derived fluorescence detected through 660 nm bandpass filter.

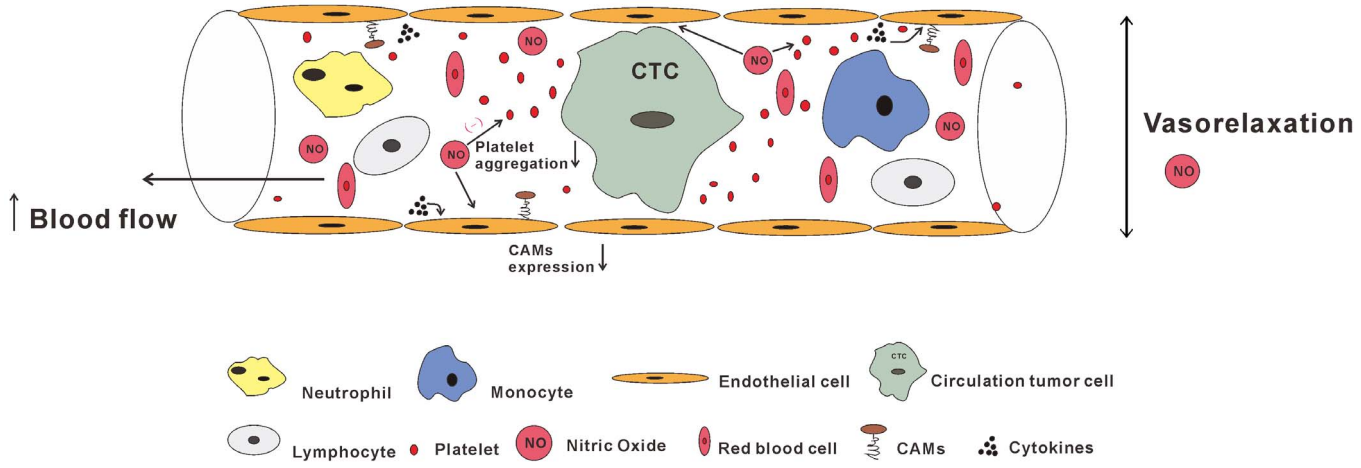

Figure 8 | Mechanisms of action by which CAP-NO inhibits adhesion of CTCs to vascular endothelium. CAP-NO makes direct vasorelaxation, increases blood flow, inhibits platelet activation and aggregation. As a result, CAP-NO interfered with the hetero-adhesion between CTCs and vascular endothelial cells by down-regulation of CAMs expression induced by cytokines. A series of beneficial effects of CAP-NO in preventing CTCs from adhesion, invasion to endothelial bed and the resultant micrometastatic foci may attribute to its collective actions.

Immunoglobulin conjugates matched for isotype and fluorochrome were used as controls to assess autofluorescence and non-specific staining.

HUVECs identification. Cell morphology was observed under a microscope. CD31 and CD144 expression was employed to determine purity of the HUVECs by flow cytometry. A total of 5×10^5 cells per tube were incubated with mouse anti-human CD144-PE and mouse anti-human CD31-FITC respectively. Background staining was performed by staining cells with PE mouse IgG1 kappa isotype control and FITC mouse IgG1 kappa isotype control, respectively. The HUVECs were incubated at 4°C for 20 min in the dark. After washing with staining buffer (phosphate buffered saline (PBS) containing 2% FBS), the HUVECs were resuspended in 500 μL of staining buffer. Flow cytometric analysis was carried out on the FACSAriaIII, and the obtained data were analyzed with FlowJo software.

Activation of adhesion molecules on HUVECs. The HUVECs were grown to confluence on 6-well tissue culture plates in fresh medium (without ECGS). Each well was stimulated differently with IFN-γ (1 ng/mL), ECGS (1 ng/mL), fibronectin (1 ng/mL), IL-6 (1 ng/mL), TNF-β (1 ng/mL), IL-1β (1 ng/mL) and TNF-α (1 ng/mL) for 4 h. The cells were collected. For each staining, expression of cell-surface ICAM-1, VCAM-1 and E-selectin was measured by flow cytometry. The HUVECs were incubated with mouse anti-human CD54-PE, mouse anti-human CD106-PE and mouse anti-human CD62E-APC antibody respectively. Background staining and purity analysis for HUVECs were determined as mentioned above.

Adhesion assay. Fluorescence-based analysis was used to evaluate effects of CAP-NO on the hetero-adhesion. HUVECs grown to confluence in 24-well tissue culture plates were pretreated with IL-1β (1 ng/mL) for 4 h. Rhodamine 123-labeled HT-29 cells were co-cultured with the HUVECs monolayers in each well, followed by treatment with CAP-NO or CAP for 1 h. After incubation, non-adhered HT-29 cells were removed by washing three times (drop-to-drop) with 1 mL PBS. We randomly selected 20 visual fields for each well and took pictures under a fluorescence microscope (Zeiss, Germany). The mean inhibition of adhesion for 20 visual fields was calculated by using the equation: % of control adhesion = [the number of adhered cells in treated samples/the number of adhered cells in the control group] × 100%, as previously described[49].

Cytotoxicity assay. Cell viability was examined by the 3-(4, 5-dimethylthiazol-2-yl)-2, 5-diphenyltetrazolium bromide (MTT) assay as previously described[25]. HT-29 cells (10^4 per well) were cultivated in McCOY's 5A medium and HUVECs (10^4 per well) were cultivated in M199 medium for 24 h. Then the supernatant was replaced with the medium containing CAP-NO from 0.1–1000 μM. After 24 h incubation, ten-μL of MTT (5 mg/mL) was added to 90 μL of the medium, and the mixture was incubated at 37°C for 4 h. The medium was then removed and 200 μL of dimethyl sulphoxide (DMSO) were added to each well. Cell viability was determined by detecting the absorbance at 570 nm in a microquant plate reader (Thermo Fisher), and the results were expressed as the cell viability ratio relative to the untreated control.

Cell cycle analysis. Cell cycle was analyzed by flow cytometry for DNA content as previously described[50]. The HT29 cell activity expressed as cell cycle distribution was determined by flow cytometry after incubation with CAP-NO (0, 1, 10 and 100 μM) for 24 h. The cells were washed with ice-cold PBS, resuspended in 200 μL of ice-cold PBS, and gently mixed with 800 μL of cold ethanol followed by incubation at 4°C overnight. The cells were washed with PBS and resuspended in 500 μL of PBS. RNAse (100 μg/mL), PI (100 μg/mL) and 0.2% Triton-X-100 were added. The cells were incubated at room temperature and protected from light for 45 min. Cell cycle was assessed by using the FACSAriaIII flow cytometer and analyzed by using the Modfit software.

Mitochondrial membrane potential measurements. $\Delta\psi_m$ was measured by the flow cytometry using the fluorescent dye DiOC6 (3). HT-29 cells were incubated with CAP-NO (0, 1, 10, 100 and 1000 μM) for 12 h. Cells were harvested and washed with ice-cold PBS, and incubated with 5 μM of DiOC6 (3) at room temperature for 20 min in the dark. The $\Delta\psi_m$ was assessed on 10,000 cells per sample by the FACSAriaIII flow cytometer. The data were processed by FlowJo software and expressed as the mean fluorescent intensities.

Flow cytometry-based adhesion assay. HUVECs were grown to confluence on 6-well tissue culture plates in fresh medium (without ECGS), and then pretreated with IL-1β (1 ng/mL) for 4 h, and then CAP-NO or CAP was added to the medium, and the cells were collected for staining. Expression of cell-surface E-selectin, ICAM-1 and VCAM-1 was measured by flow cytometry. HT-29 cells were grown on 6-well tissue culture plates followed by treatment with CAP-NO (1–100 μM) for 1, 4 and 12 h. The cell-surface adhesion ligand CD29 was then measured by flow cytometry. The cells and primary antibodies were incubated at 4°C for 20 min in the dark. After washing with staining buffer, the cell suspension was passed through the flow cell of the FACSAriaIII flow cytometer for analysis. The data were processed by FlowJo software and expressed as the mean fluorescent intensities.

Western blot analysis. To induce the expression of VCAM-1, HUVECs were incubated with fresh media (without ECGS), and pretreated with IL-1β (1 ng/mL) or IFN-γ (10 ng/mL) for 4 h, followed by treatment of the HUVECs with CAP-NO for 12 h. After cell lysis, equal volumes (20 μL per lane) of protein were separated by sodium dodecylsulfate-polyacrylamide gel electrophoresis (SDS-PAGE, Bio-Rad), and transferred to polyvinylidene difluoride (PVDF, Bio-Rad) membrane. The membranes were blocked in 5% skim milk for 1 h at room temperature and then incubated with the following primary antibodies overnight at 4°C: anti-VCAM-1 (1 : 800 dilution), anti-β-actin (1 : 1,000 dilution) as the loading control. After washing, the membranes were incubated with the following secondary antibodies for 1 h at room temperature: goat anti-mouse secondary antibody conjugated with horseradish peroxidase (1 : 7,500 dilution, ZSGB-BIO, Beijing) or goat anti-rabbit secondary antibody conjugated with horseradish peroxidase (1 : 7,500 dilution, ZSGB-BIO, Beijing). Chemiluminescent signals were generated using a Super Signal West Pico Chemiluminescent Substrate kit (Pierce), and detected by using the ChemiDoc XRS system (Bio-Rad). Band intensity was quantified by use of Image Lab analysis software (Bio-Rad). Total VCAM-1 expression was normalized to β-actin levels.

Statistical analysis. Results were expressed as mean values ± SEM. The ANOVA was applied to examine significance of differences, and $P < 0.05$ was considered statistically significant.

1. Nguyen, D. X., Bos, P. D. & Massague, J. Metastasis: from dissemination to organ-specific colonization. *Nat Rev Cancer* **9**, 274–284 (2009).
2. Sethi, N. & Kang, Y. Unravelling the complexity of metastasis - molecular understanding and targeted therapies. *Nat Rev Cancer* **11**, 735–748 (2011).
3. Plaks, V., Koopman, C. D. & Werb, Z. Cancer. Circulating tumor cells. *Science* **341**, 1186–1188 (2013).
4. Chaffer, C. L. & Weinberg, R. A. A perspective on cancer cell metastasis. *Science* **331**, 1559–1564 (2011).
5. Alby, L. & Auerbach, R. Differential adhesion of tumor cells to capillary endothelial cells in vitro. *Proc Natl Acad of Sci USA* **81**, 5739–5743 (1984).
6. Dejana, E. *et al.* Interleukin 1 promotes tumor cell adhesion to cultured human endothelial cells. *J Clin Invest* **82**, 1466 (1988).
7. Rice, G. E. & Bevilacqua, M. P. An inducible endothelial cell surface glycoprotein mediates melanoma adhesion. *Science* **246**, 1303–1306 (1989).
8. Meager, A. Cytokine regulation of cellular adhesion molecule expression in inflammation. *Cytokine Growth Factor Rev* **10**, 27–39 (1999).
9. Taichman, D. *et al.* Tumor cell surface alpha 4 beta 1 integrin mediates adhesion to vascular endothelium: demonstration of an interaction with the N-terminal domains of INCAM-110/VCAM-1. *Cell Regul* **2**, 347 (1991).
10. Phillips, M. L. *et al.* ELAM-1 mediates cell adhesion by recognition of a carbohydrate ligand, sialyl-Lex. *Science* **250**, 1130–1132 (1990).
11. Zen, K. *et al.* CD44v4 is a major E-selectin ligand that mediates breast cancer cell transendothelial migration. *PLoS One* **3**, e1826 (2008).
12. Honn, K. V. & Tang, D. G. Adhesion molecules and tumor cell interaction with endothelium and subendothelial matrix. *Cancer Metastasis Rev* **11**, 353–375 (1992).
13. Lauri, D., Needham, L., Martin-Padura, I. & Dejana, E. Tumor cell adhesion to endothelial cells: endothelial leukocyte adhesion molecule-1 as an inducible adhesive receptor specific for colon carcinoma cells. *J Natl Cancer Inst* **83**, 1321–1324 (1991).
14. Takada, A. *et al.* Contribution of carbohydrate antigens sialyl Lewis A and sialyl Lewis X to adhesion of human cancer cells to vascular endothelium. *Cancer Res* **53**, 354–361 (1993).
15. Furchgott, R. F. & Zawadzki, J. V. The obligatory role of endothelial cells in the relaxation of arterial smooth muscle by acetylcholine. *Nature* **288**, 373–376 (1980).
16. Palmer, R. M., Ferrige, A. G. & Moncada, S. Nitric oxide release accounts for the biological activity of endothelium-derived relaxing factor. *Nature* **327**, 524–526 (1987).
17. Loscalzo, J. Nitric oxide insufficiency, platelet activation, and arterial thrombosis. *Circ Res* **88**, 756–762 (2001).
18. Jia, L. & Stamler, J. S. Dual actions of S-nitrosylated derivative of vasoactive intestinal peptide as a vasoactive intestinal peptide-like mediator and a nitric oxide carrier. *Eur J Pharmacol* **366**, 79–86 (1999).
19. Jia, L. & Wong, H. In vitro and in vivo assessment of cellular permeability and pharmacodynamics of S-nitrosylated captopril, a nitric oxide donor. *Br J Pharmacol* **134**, 1697–1704 (2001).
20. Nakaki, T., Nakayama, M. & Kato, R. Inhibition by nitric oxide and nitric oxide-producing vasodilators of DNA synthesis in vascular smooth muscle cells. *Eur J Pharmacol* **189**, 347–353 (1990).
21. Kubes, P., Suzuki, M. & Granger, D. Nitric oxide: an endogenous modulator of leukocyte adhesion. *Proc Natl Acad of Sci USA* **88**, 4651–4655 (1991).
22. Tsao, P. S., McEvoy, L. M., Drexler, H., Butcher, E. C. & Cooke, J. P. Enhanced endothelial adhesiveness in hypercholesterolemia is attenuated by L-arginine. *Circulation* **89**, 2176–2182 (1994).
23. Jia, L. *et al.* Effect of nitric oxide on cytotoxicity of Taxol: enhanced Taxol transcellular permeability. *Biochem Pharmacol* **66**, 2193–2199 (2003).
24. Xu, W., Liu, L. Z., Loizidou, M., Ahmed, M. & Charles, I. G. The role of nitric oxide in cancer. *Cell Res* **12**, 311–320 (2002).
25. Jia, L. & Blantz, R. C. The effects of S-nitrosocaptopril on renal filtration and blood pressure in rats. *Eur J Pharmacol* **354**, 33–41 (1998).

26. Loscalzo, J., Smick, D., Andon, N. & Cooke, J. S-nitrosocaptopril. I. Molecular characterization and effects on the vasculature and on platelets. *J Pharmacol Exp Ther* **249**, 726–729 (1989).
27. Lin, M., Yang, X., Wang, J., Jia, B. & Jia, L. Inhibitory effects of S-nitrosocaptopril on vasomotor tone. *Acta Pharmacol Sin* **19**, 485 (1998).
28. Tsui, D. Y., Gambino, A. & Wanstall, J. C. S-nitrosocaptopril: in vitro characterization of pulmonary vascular effects in rats. *Br J Pharmacol* **138**, 855–864 (2003).
29. Jia, L. & Furchgott, R. F. Inhibition by sulfhydryl compounds of vascular relaxation induced by nitric oxide and endothelium-derived relaxing factor. *J Pharmacol Exp Ther* **267**, 371–378 (1993).
30. Furchgott, R. F. The 1996 Albert Lasker Medical Research Awards. The discovery of endothelium-derived relaxing factor and its importance in the identification of nitric oxide. *JAMA* **276**, 1186–1188 (1996).
31. Jaffe, E. A., Nachman, R. L., Becker, C. G. & Minick, C. R. Culture of human endothelial cells derived from umbilical veins. Identification by morphologic and immunologic criteria. *J Clin Invest* **52**, 2745–2756 (1973).
32. Peichev, M. *et al.* Expression of VEGFR-2 and AC133 by circulating human CD34+ cells identifies a population of functional endothelial precursors. *Blood* **95**, 952–958 (2000).
33. Ricci-Vitiani, L. *et al.* Tumour vascularization via endothelial differentiation of glioblastoma stem-like cells. *Nature* **468**, 824–828 (2010).
34. Miettinen, M., Lindenmayer, A. E. & Chaubal, A. Endothelial cell markers CD31, CD34, and BNH9 antibody to H- and Y-antigens--evaluation of their specificity and sensitivity in the diagnosis of vascular tumors and comparison with von Willebrand factor. *Mod Pathol* **7**, 82–90 (1994).
35. Bevilacqua, M. P., Pober, J. S., Wheeler, M. E., Cotran, R. S. & Gimbrone Jr, M. A. Interleukin 1 acts on cultured human vascular endothelium to increase the adhesion of polymorphonuclear leukocytes, monocytes, and related leukocyte cell lines. *J Clin Invest* **76**, 2003–2011 (1985).
36. Amano, M., Takahashi, M., Kosaka, T. & Kinoshita, M. Differential inhibition of platelet aggregation and calcium mobilization by nitroglycerin and stabilized nitric oxide. *J Cardiovasc Pharmacol* **24**, 860–866 (1994).
37. Cooke, J. P., Andon, N. & Loscalzo, J. S-nitrosocaptopril. II. Effects on vascular reactivity. *J Pharmacol Exp Ther* **249**, 730–734 (1989).
38. Nakae, I., Takahashi, M., Kinoshita, T., Matsumoto, T. & Kinoshita, M. The effects of S-nitrosocaptopril on canine coronary circulation. *J Pharmacol Exp Ther* **274**, 40–46 (1995).
39. Shaffer, J. E. *et al.* The hemodynamic effects of S-nitrosocaptopril in anesthetized dogs. *J Pharmacol Exp Ther* **256**, 704–709 (1991).
40. Jia, L., Pei, R., Lin, M. & Yang, X. Acute and subacute toxicity and efficacy of S-nitrosylated captopril, an ACE inhibitor possessing nitric oxide activities. *Food Chem Toxicol* **39**, 1135–1143 (2001).
41. Jia, L., Wu, C. C., Guo, W. & Young, X. Antiangiogenic effects of S-nitrosocaptopril crystals as a nitric oxide donor. *Eur J Pharmacol* **391**, 137–144 (2000).
42. Tsao, P. S., Buitrago, R., Chan, J. R. & Cooke, J. P. Fluid flow inhibits endothelial adhesiveness nitric oxide and transcriptional regulation of VCAM-1. *Circulation* **94**, 1682–1689 (1996).
43. De Caterina, R. *et al.* Nitric oxide decreases cytokine-induced endothelial activation. Nitric oxide selectively reduces endothelial expression of adhesion molecules and proinflammatory cytokines. *J Clin Invest* **96**, 60 (1995).
44. Jordan, B. F. *et al.* Captopril and S-nitrosocaptopril as potent radiosensitizers: Comparative study and underlying mechanisms. *Cancer Lett* **293**, 213–219 (2010).
45. Gay, L. J. & Felding-Habermann, B. Contribution of platelets to tumour metastasis. *Na Rev Cancer* **11**, 123–134 (2011).
46. Jia, L. *et al.* EDRF-like activity and anticancer spectrum of JS-K, a novel diazeniumdiolate nitric oxide donor. In: *Proc. Am. Assoc. Cancer Res* **44**, 1059 (2003).
47. Jia, L., Young, X. & Guo, W. Physicochemistry, pharmacokinetics, and pharmacodynamics of S-nitrosocaptopril crystals, a new nitric oxide donor. *J Pharm Sci* **88**, 981–986 (1999).
48. Garthwaite, J. *et al.* Potent and selective inhibition of nitric oxide-sensitive guanylyl cyclase by 1H-[1,2,4]oxadiazolo[4,3-a]quinoxalin-1-one. *Mol Pharmacol* **48**, 184–188 (1995).
49. Wang, J. *et al.* Synthesis, Spectral Characterization, and In Vitro Cellular Activities of Metapristone, a Potential Cancer Metastatic Chemopreventive Agent Derived from Mifepristone (RU486). *AAPS J*, DOI: 10.1208/s12248-013-9559-2 (2014).
50. Shao, J. *et al.* Intracellular distribution and mechanisms of actions of photosensitizer Zinc(II)-phthalocyanine solubilized in Cremophor EL against human hepatocellular carcinoma HepG2 cells. *Cancer Lett* **330**, 49–56 (2013).

Acknowledgments

This research was supported by the National Natural Science Foundation of China (NSFC) grant 81273548 and 81201709.

Author contributions

L.J., J.S. and Y.L. conceived and designed the experiments. Y.L., T.Y. and H.L. performed the flow cytometry-based adhesion experiments. Y.L., T.Y., H.L., J.W., J.X. and S.C. performed cell culture and western blot experiments. Y.L., T.Y., H.L. and S.Y. acquired and analyzed the experimental data. L.W., Y.G. and J.S. provided essential reagents and critical comments. L.J. and Y.L. wrote the manuscript. All authors reviewed the manuscript.

Additional information

Supplementary information accompanies this paper at http://www.nature.com/scientificreports

Competing financial interests: The authors declare no competing financial interests.

How to cite this article: Lu, Y.S. *et al.* Nitric Oxide Inhibits Hetero-adhesion of Cancer Cells to Endothelial Cells: Restraining Circulating Tumor Cells from Initiating Metastatic Cascade. *Sci. Rep.* **4**, 4344; DOI:10.1038/srep04344 (2014).